

**Transport properties in normal-metal  $\text{Bi}_2\text{Pd}_3\text{S}_2$  and superconducting  $\text{Bi}_2\text{Pd}_3\text{Se}_2$** 

Takeshi Sakamoto, Makoto Wakeshima,\* and Yukio Hinatsu

*Division of Chemistry, Graduate School of Science, Hokkaido University, Sapporo 060-0810, Japan*

Kazuyuki Matsuhira

*Department of Electronics, Faculty of Engineering, Kyushu Institute of Technology, Kitakyushu 804-8550, Japan*

(Received 16 April 2008; published 9 July 2008)

The transport properties of the parkerite-related compounds  $\text{Bi}_2\text{Pd}_3\text{X}_2$  ( $X=\text{S,Se}$ ) were studied. The electrical resistivities of both compounds show typical metallic behavior up to 400 K. Resistivity and specific heat measurements at low temperatures reveal that  $\text{Bi}_2\text{Pd}_3\text{Se}_2$  is superconducting below 1 K. On the other hand,  $\text{Bi}_2\text{Pd}_3\text{S}_2$  does not show a bulk superconducting transition down to 0.35 K. In the normal state, the electronic specific heat coefficient  $\gamma$  and the Debye temperature  $\Theta_D$  are found to be 5.9 mJ/mol K<sup>2</sup> and 170 K, respectively for  $\text{Bi}_2\text{Pd}_3\text{S}_2$ , and 8.3 mJ/mol K<sup>2</sup> and 150 K, respectively for  $\text{Bi}_2\text{Pd}_3\text{Se}_2$ . In the superconducting state for  $\text{Bi}_2\text{Pd}_3\text{Se}_2$ , the upper critical field at zero temperature for  $\text{Bi}_2\text{Pd}_3\text{Se}_2$  is 290 mT. From the electronic specific heat in the superconducting temperature range, it was found that  $\text{Bi}_2\text{Pd}_3\text{Se}_2$  belongs to an *s*-wave weak-coupling superconductor.

DOI: [10.1103/PhysRevB.78.024509](https://doi.org/10.1103/PhysRevB.78.024509)

PACS number(s): 74.25.Fy, 72.15.Eb

**I. INTRODUCTION**

Transition-metal chalcogenides have been of interest in chemistry and materials science because of their exceptional physical and chemical properties such as charge-density-wave behavior, superconductivity, and intercalation reactions. In addition, striking structures are observed in the mixed metal-rich chalcogenides, which form a wide variety of heterometallic bonds ranging from one-dimensional (1D) chains in  $\text{Sc}_{14}\text{M}_3\text{Te}_8$  ( $M=\text{Ru,Os}$ ) (Ref. 1), 2D slabs in  $\text{Ni}_6\text{SnS}_2$  and  $\text{Ni}_9\text{Sn}_2\text{S}_2$  (Ref. 2), and 3D frameworks  $\text{Ta}_9\text{M}_2\text{S}_6$  ( $M=\text{Fe,Co,Ni}$ ) (Ref. 3).

Ternary-metal-rich chalcogenides  $\text{Bi}_2\text{M}_3\text{X}_2$  ( $M=\text{Ni,Rh,Pd}$ ;  $X=\text{S,Se}$ ) crystallize in the parkerite-type structure.<sup>4–6</sup> Recently, the detailed crystal structure for parkerite  $\text{Bi}_2\text{Ni}_3\text{S}_2$  was reported from its single-crystal x-ray diffraction analysis.<sup>7</sup> The structure can be represented as a 3D framework formed by the strong heterometallic Ni-Bi and Ni-S bonds. At the same time, very weak Ni-Ni bonds also exist. On the physical properties of parkerite-related compounds, only the results of resistivity and thermopower measurements above liquid-nitrogen temperature were reported.<sup>6</sup>

In our previous study, it was found that the parkerite-related nickel chalcogenides  $\text{Bi}_2\text{Ni}_3\text{S}_2$  and  $\text{Bi}_2\text{Ni}_3\text{Se}_2$  had slightly different crystal structures. Both compounds showed a superconducting transition ( $T_c \sim 0.7$  K) through their electrical resistivity and specific heat measurements.<sup>8</sup> Furthermore, we reported that a new rhodium selenide  $\text{Bi}_2\text{Rh}_3\text{Se}_2$  exhibited a charge-density-wave (CDW) transition around 240 K in addition to a superconducting transition ( $T_c \sim 0.7$  K).<sup>9</sup> In the case of  $\text{Bi}_2\text{Rh}_3\text{Se}_2$ , it is suggested that a pseudo-2D Fermi surface, which is formed by strong 2D Rh-Rh bonds, yields a CDW state below 240 K from the calculation of the electronic structure using the full-potential linearized augmented plane wave + local orbitals (FP-LAPW + lo) method.

In order to investigate the interesting electronic properties of the parkerite-type compounds, we have carried out electrical resistivity, thermoelectric power, and specific heat mea-

surements of palladium chalcogenides  $\text{Bi}_2\text{Pd}_3\text{X}_2$  ( $X=\text{S,Se}$ ). For only the  $\text{Bi}_2\text{Pd}_3\text{Se}_2$ , a superconducting transition was observed. Their results will be reported here.

**II. EXPERIMENT**

The samples were prepared from stoichiometric mixtures of the following elements: Bi powder (99.9%), Pd powder (99.95%), S powder (99.99%), and Se powder (99.9%). The mixtures were pressed into pellets and then sealed in an evacuated quartz tube. To avoid a reaction between the samples and the quartz tube, the tube was coated with carbon. The samples were heated at 1270 K for 12 h and rapidly to room temperature hereafter.

Powder x-ray diffraction measurements were carried out in the region of  $10^\circ \leq 2\theta \leq 120^\circ$  using Cu  $K\alpha$  radiation on a Rigaku RINT 2000 diffractometer equipped with a curved graphite monochromator. The crystal structures were determined by the Rietveld technique, using the program RIETAN 2000.<sup>10</sup>

Electrical resistivity measurements were carried out in the temperature range of 0.35–400 K and in magnetic fields up to 400 mT by the standard four-probe method with using a Quantum Design physical-property-measurement system (PPMS) equipped with a <sup>3</sup>He refrigerator. The sintered samples were cut into pieces having sizes of approximately  $5 \times 2 \times 0.7$  mm<sup>3</sup> ( $\text{Bi}_2\text{Pd}_3\text{S}_2$ ) and  $4 \times 2 \times 1$  mm<sup>3</sup> ( $\text{Bi}_2\text{Pd}_3\text{Se}_2$ ). Four contact wires were painted onto the samples using silver paste.

The thermoelectric power (TEP) was measured by a differential method using Au–0.07% Fe versus Chromel thermocouples in the temperature range between 10 K and 300 K.

Specific heat measurements were performed by thermal relaxation in the temperature range between 0.35 K and 15 K with the PPMS. The sintered samples ( $\sim 15$  mg) were mounted on a thin alumina plate with Apiezon N grease for better thermal contact.

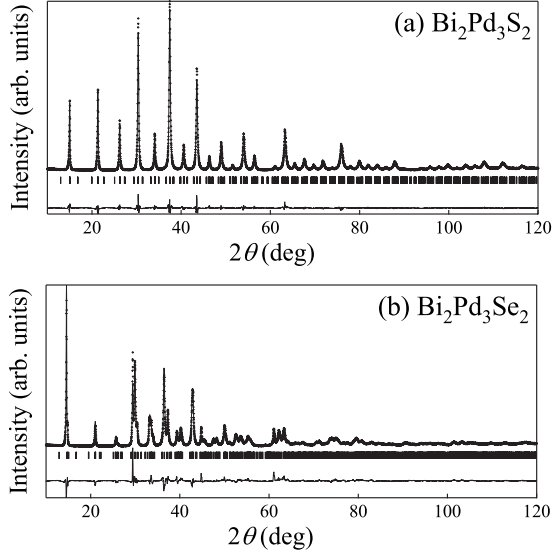


FIG. 1. X-ray diffraction profiles for (a)  $\text{Bi}_2\text{Pd}_3\text{S}_2$  and (b)  $\text{Bi}_2\text{Pd}_3\text{Se}_2$ .

### III. RESULTS AND DISCUSSION

#### A. X-ray powder diffraction

The  $\text{Bi}_2\text{Pd}_3\text{X}_2$  ( $X=\text{S},\text{Se}$ ) phases are identified from the x-ray diffraction (XRD) profiles. The x-ray diffraction profiles for  $\text{Bi}_2\text{Pd}_3\text{S}_2$  and  $\text{Bi}_2\text{Pd}_3\text{Se}_2$  are shown in Figs. 1(a) and 1(b), respectively. The profile for  $\text{Bi}_2\text{Pd}_3\text{X}_2$  is indexed with a monoclinic parkerite-type cell with the space group  $C2/m$ . By a Rietveld analysis, the crystallographic parameters of  $\text{Bi}_2\text{Pd}_3\text{S}_2$  were refined as the initial values using those of the  $\text{Bi}_2\text{Ni}_3\text{S}_2$ -type structure<sup>8</sup> and its calculated XRD profile is in good agreement with the observed one (the reliability factors are 9.1% for  $R_{\text{wp}}$  and 2.07% for  $R_I$ ). The lattice parameters were refined to be  $a=11.751(1)$  Å,  $b=8.303(1)$  Å,  $c=11.740(2)$  Å, and  $\beta=89.96(1)^\circ$ . The positional parameters are listed in Table I.

However, the  $R$  factors for  $\text{Bi}_2\text{Pd}_3\text{Se}_2$  are comparatively large ( $R_{\text{wp}}=13.7\%$  and  $R_I=5.31\%$ ) and a disagreement be-

TABLE I. Crystal structure data for  $\text{Bi}_2\text{Pd}_3\text{S}_2$ .

Atom	$x$	$y$	$z$	$B$ (Å)
Bi(1)	0.123(1)	0	0.370(1)	0.85(4)
Bi(2)	0.375(1)	0	0.133(3)	0.85
Bi(3)	0.625(2)	0	0.380(1)	0.85
Bi(4)	0.570(2)	0	0.114(1)	0.85
Pd(1)	1/4	3/4	0	1.02(6)
Pd(2)	1/4	1/4	1/2	1.02
Pd(3)	1/2	-0.274(3)	1/2	1.02
Pd(4)	0	-0.266(3)	0	1.02
Pd(5)	0.400(3)	0	0.363(3)	1.02
Pd(6)	0.109(3)	0	0.149(2)	1.02
S(1)	0.391(3)	-0.282(9)	0.353(5)	0.8
S(2)	0.108(3)	-0.283(8)	0.145(5)	0.8

tween the observed and calculated profiles is found for several diffraction peaks, which suggests that the structure of  $\text{Bi}_2\text{Pd}_3\text{Se}_2$  is not the same as that of  $\text{Bi}_2\text{Pd}_3\text{S}_2$ . A similar difference in the crystal structures between sulfide and selenide is found in  $\text{Bi}_2\text{Ni}_3\text{S}_2$  and  $\text{Bi}_2\text{Ni}_3\text{Se}_2$ .<sup>8,11</sup>

#### B. Physical properties

Figure 2(a) shows the temperature dependence of the electrical resistivity for  $\text{Bi}_2\text{Pd}_3\text{S}_2$ . Above 0.8 K, the resistivity increases monotonously with temperature up to 400 K, which indicates a typical metallic conductivity. Around 0.6 K, the resistivity shows a superconducting phase transition. However, this transition is not observed for the specific heat measurement as will be described later; thus, this anomaly is supposed to be caused by a superconducting impurity which is an undetectable phase in the x-ray diffraction profile.

Figure 2(b) shows the temperature dependence of the electrical resistivity for  $\text{Bi}_2\text{Pd}_3\text{Se}_2$ . This compound also shows typical metallic behavior up to 400 K. The resistivity as a function of temperature below 1.5 K is plotted in the inset of Fig. 2(b). Below 1.1 K, the resistivity drops abruptly, indicating a phase transition to a superconducting state.

Figure 2(c) shows the temperature dependence of TEP for  $\text{Bi}_2\text{Pd}_3\text{Se}_2$ . It can be seen that the thermopower of  $\text{Bi}_2\text{Pd}_3\text{Se}_2$  is negative over the whole temperature range and the thermopower  $S$  has approximately a linear relationship with temperature above 100 K. These results indicate that this compound is a typical metallic one. Below 50 K,  $S$  drops with decreasing temperature and this drop would result from the phonon-drag effect. The total  $S$  is represented by the relation

$$S = S_d + S_p, \quad (1)$$

where  $S_d$  and  $S_p$  are the diffusion thermoelectric power and the contribution from the phonon drag, respectively. The diffusion thermoelectric power  $S_d$  is represented as  $-(\pi^2 k_B^2 T / 3 |e|) [dN(\epsilon) / d\epsilon]$  in the simplest free-electron model with the density states  $N(\epsilon)$  near the Fermi level  $\epsilon_F$ . The contribution of the phonon drag is described by<sup>12</sup>

$$S_p = \left( \frac{T}{\Theta_D} \right)^3 \int_0^{T/\Theta_D} \frac{x^4 \exp x}{(\exp x - 1)^2} \alpha(x) dx,$$

$$\alpha(x) = \frac{1}{1 + \tau_{pe}/\tau_{pp}} = \frac{1}{1 + 2 \times 10^{-6} \exp(-\beta/T)x^2 T^3}, \quad (2)$$

where  $\tau_{pe}$  and  $\tau_{pp}$  are the relaxation time for phonon-electron interaction and the relaxation time for phonon-phonon interaction, respectively. The theoretical curve with the Debye temperature  $\Theta_D=150$  K [solid line in Fig. 3(c)] using Eq. (1) is in good agreement with the experimental data. This value of  $\Theta_D$  is consistent with the value of  $\Theta_D=150$  K obtained from the specific heat measurement as will be described later.

Figure 3(a) shows the temperature dependence of resistivities in various magnetic fields. The resistivity in the zero field drops sharply, indicating a phase transition to a superconducting state. The onset temperature is 1.1 K, and zero resistivity is attained below 0.9 K. The critical temperature

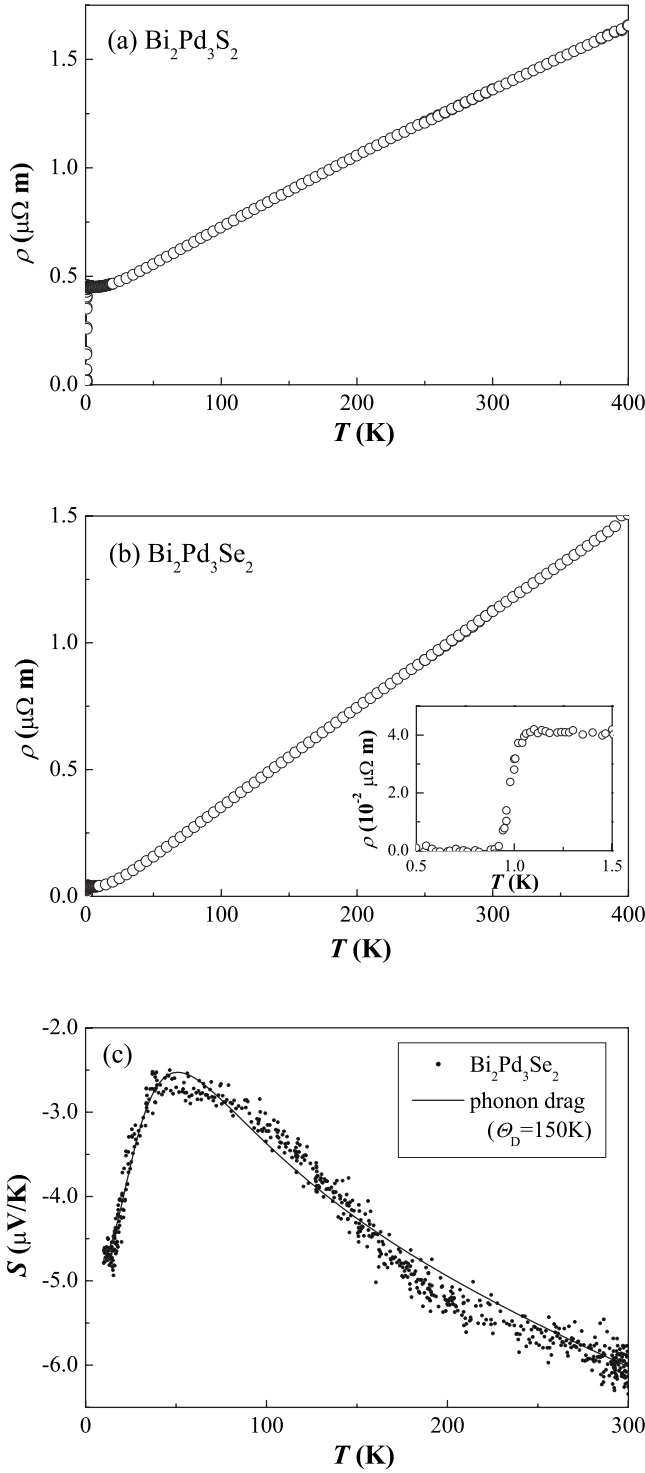


FIG. 2. (a) Temperature dependence of the electrical resistivity for Bi<sub>2</sub>Pd<sub>3</sub>S<sub>2</sub>. (b) Temperature dependence of the electrical resistivity for Bi<sub>2</sub>Pd<sub>3</sub>Se<sub>2</sub>. (c) Thermoelectric power as a function of temperature for Bi<sub>2</sub>Pd<sub>3</sub>Se<sub>2</sub>. The solid line shows fitting results using Eq. (1).

$T_c$  is defined as the midpoint of the transition;  $T_c^{\text{mid},R} = 0.96$  K. Figure 3(b) shows the field dependence of resistivities at various temperatures. The values of  $T_c^{\text{mid},R}$  decrease with increasing applied field as shown in Figs. 3(a) and 3(b). Assuming that Bi<sub>2</sub>Pd<sub>3</sub>Se<sub>2</sub> is a type-II superconductor, as will

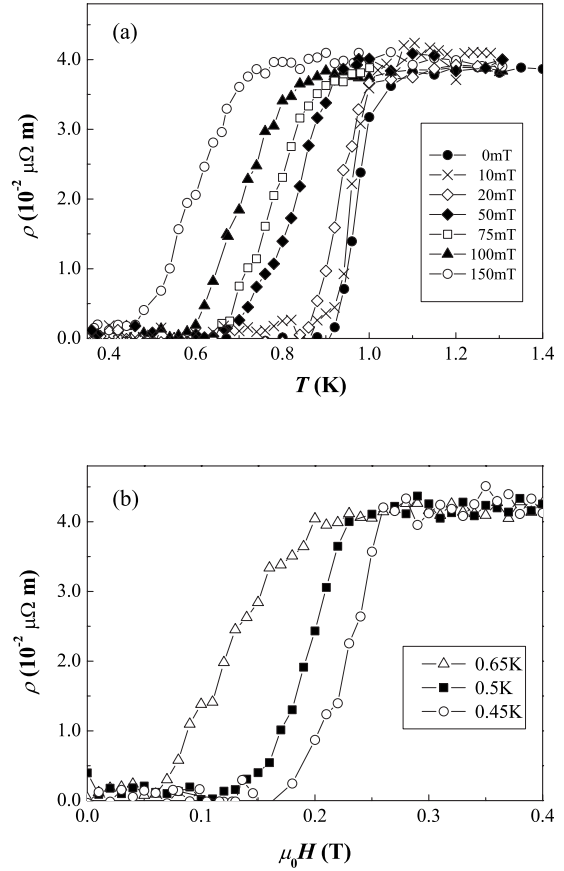


FIG. 3. (a) Temperature dependence of the electrical resistivity under various magnetic fields for Bi<sub>2</sub>Pd<sub>3</sub>Se<sub>2</sub>. (b) Magnetic field dependence of electrical resistivity at various temperatures for Bi<sub>2</sub>Pd<sub>3</sub>Se<sub>2</sub>.

be justified below, the upper critical fields  $\mu_0 H_{c2}(T)$  were determined from Figs. 3(a) and 3(b).

Figure 4 shows  $\mu_0 H_{c2}(T)$  as a function of the critical temperature. According to the Werthamer-Helfand-Hohenberg (WHH) theory for a type-II superconductor in the dirty limit,<sup>13</sup> the upper critical field at zero temperature can be estimated from the relation

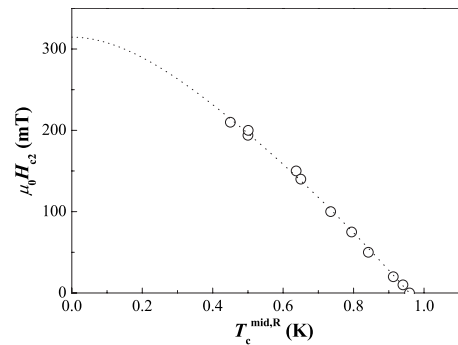


FIG. 4. Temperature dependence of the upper critical field for Bi<sub>2</sub>Pd<sub>3</sub>Se<sub>2</sub> determined from the electrical resistivity data. Dotted lines show the fitting results using the WHH theory.

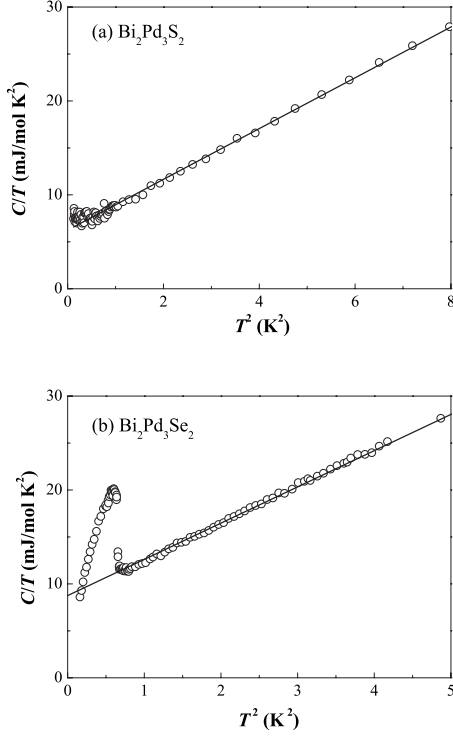


FIG. 5. Temperature dependences of the specific heat  $C$  divided by temperature for (a)  $\text{Bi}_2\text{Pd}_3\text{S}_2$  and (b)  $\text{Bi}_2\text{Pd}_3\text{Se}_2$ .

$$\mu_0 H_{c2}(0) = -0.693 T_c \left( \frac{d\mu_0 H_{c2}(T)}{dT} \right)_{T \sim T_c}. \quad (3)$$

The gradient  $d\mu_0 H_{c2}(T)/dT$  in the linear region near  $T_c$  of  $\text{Bi}_2\text{Pd}_3\text{Se}_2$  is found to be about  $-473$  mT/K. Consequently, the  $\mu_0 H_{c2}(0)$  values are found to be about 315 mT. Moreover, the values of the Ginzburg-Landau (GL) coherence length at zero temperature,  $\xi_{\text{GL}}(0)$ , can be estimated to be 323 Å by the following formula,

$$\mu_0 H_{c2}(0) = \frac{\Phi_0}{2\pi \xi_{\text{GL}}(0)^2}, \quad (4)$$

where  $\Phi_0$  is the quantum flux.

The temperature dependences of the specific heat,  $C$ , divided by temperature for  $\text{Bi}_2\text{Pd}_3\text{S}_2$  and  $\text{Bi}_2\text{Pd}_3\text{Se}_2$  are shown in Figs. 5(a) and 5(b), respectively. For  $\text{Bi}_2\text{Pd}_3\text{S}_2$ , the  $C_p/T-T^2$  plot shows no anomaly down to 0.35 K. Thus, the superconducting phase transition observed in the  $\rho$ - $T$  plot [Fig. 2(a)] is not a nature originated from the bulk of  $\text{Bi}_2\text{Pd}_3\text{S}_2$ . For  $\text{Bi}_2\text{Pd}_3\text{Se}_2$ , the fact that a jump in the specific heat is observed starting at 0.83 K is indicative of the bulk superconducting transition. The critical temperature from specific heat data defined as the midpoint of the transition ( $T_c^{\text{mid},C}$ ) is determined to be 0.81 K for  $\text{Bi}_2\text{Pd}_3\text{Se}_2$ .

We assume that the total specific heat is composed of the electron and lattice parts  $C(T) = C_e(T) + C_{\text{ph}}(T)$ . In the normal state, the lattice part is expressed by the  $\beta T^3$  term at the temperature much below the Debye temperature  $\Theta_D$  and the electronic specific heat is assumed to be the  $\gamma T$  term—i.e.,

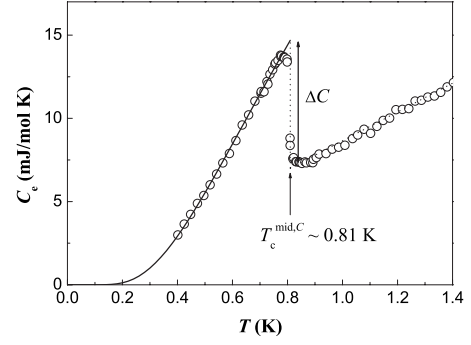


FIG. 6. Temperature dependence of the electronic specific heat for  $\text{Bi}_2\text{Pd}_3\text{Se}_2$ . The solid lines show fitting results using exponential functions.

$$C_p/T = \gamma + \beta T^2. \quad (5)$$

From the  $C(T)/T$  versus  $T^2$  plot, the  $\gamma$  and  $\beta$  values of both compounds were obtained to be 5.9 mJ/mol K<sup>2</sup> and 2.7 mJ/mol K<sup>4</sup> for  $\text{Bi}_2\text{Pd}_3\text{S}_2$  and 8.3 mJ/mol K<sup>2</sup> and 4.0 mJ/mol K<sup>4</sup> for  $\text{Bi}_2\text{Pd}_3\text{Se}_2$ . The values of  $\Theta_D$  were then calculated to be 170 K ( $\text{Bi}_2\text{Pd}_3\text{S}_2$ ) and 150 K ( $\text{Bi}_2\text{Pd}_3\text{Se}_2$ ) using the formula

$$\Theta_D = \left( \frac{12nR\pi^4}{5\beta} \right)^{1/3}, \quad (6)$$

where  $R=8.314$  J/mol K and the number of elements per formula unit,  $n=7$ , for both compounds. The value of  $\gamma$  for  $\text{Bi}_2\text{Pd}_3\text{S}_2$  is small as compared with those for the parkerite-type superconductors  $\text{Bi}_2\text{Ni}_3\text{S}_2$  (11.4 mJ/mol K<sup>2</sup>),  $\text{Bi}_2\text{Ni}_3\text{Se}_2$  (12.2 mJ/mol K<sup>2</sup>) (Ref. 8), and  $\text{Bi}_2\text{Pd}_3\text{Se}_2$  (8.3 mJ/mol K<sup>2</sup>), indicative of a weak electron-phonon coupling. No superconducting transition down to 0.35 K for  $\text{Bi}_2\text{Pd}_3\text{S}_2$  would result from a weak electron-phonon coupling.

For  $\text{Bi}_2\text{Pd}_3\text{Se}_2$ , the electron-phonon coupling constant  $\lambda_{\text{e-ph}}$  is estimated from the McMillan equation for the superconducting transition temperature<sup>14</sup>

$$T_c = \frac{\Theta_D}{1.45} \exp \left[ - \frac{1.04(1 + \lambda_{\text{e-ph}})}{\lambda_{\text{e-ph}} - \mu^*(1 + 0.62\lambda_{\text{e-ph}})} \right], \quad (7)$$

where the Coulomb pseudopotential  $\mu^*$  is assumed to be 0.13 empirically. The value of  $\lambda_{\text{e-ph}}$  is determined to be 0.49. This small  $\lambda_{\text{e-ph}}$  value indicates that  $\text{Bi}_2\text{Pd}_3\text{Se}_2$  is classified into a weak electron-phonon coupling superconductor.

The electronic specific heat  $C_e$  was obtained by subtracting the lattice contribution estimated earlier from the total specific heat, and the temperature dependence of  $C_e$  for  $\text{Bi}_2\text{Pd}_3\text{Se}_2$  is plotted in Fig. 6. Below the superconducting transition temperature, the temperature dependences of the electronic specific heat cannot be fitted with a  $T^n$  function, but it follows the exponential decay as seen in Fig. 6. These fitting results show that this compound is an  $s$ -wave superconductor. The normalized specific heat jump value  $\Delta C/\gamma T_c^{\text{mid},C}$  is 1.15 for  $\text{Bi}_2\text{Pd}_3\text{Se}_2$ . This value is smaller than 1.43 expected from the BCS theory<sup>15</sup> and is close to that of isomorphous  $\text{Bi}_2\text{Ni}_3\text{Se}_2$  ( $\Delta C/\gamma T_c^{\text{mid},C}=1.16$ ). These small

jump values are comparable with those of weak-coupling BCS superconductors having an anisotropic-energy gap like Nb<sub>3</sub>X<sub>4</sub> (X=S,Se).<sup>16,17</sup> The small  $\Delta C/\gamma T_c^{\text{mid},C}$  might be attributable to such an anisotropy of crystal structures for Bi<sub>2</sub>M<sub>3</sub>Se<sub>2</sub> (M=Ni,Pd). A detailed discussion of the anisotropic-energy gap will require studies of specific heat measurements in a magnetic field using a single crystal.

The thermodynamic critical field  $\mu_0 H_c(T)$  can be obtained as a function of temperature using the specific heat data in both the normal and superconducting states. The difference in entropy  $\Delta S(T)$  between the normal and superconducting states was obtained through the thermodynamic relation

$$\Delta S(T) = S_n(T) - S_s(T) = \gamma T - \int_0^T \frac{C_{\text{es}}(T')}{T'} dT', \quad (8)$$

where  $S_n(T)$  and  $S_s(T)$  are the entropies in the normal and superconducting states and  $C_{\text{es}}$  is the electronic specific heat in the superconducting state. The  $C_{\text{es}}$  below 0.4 K is extrapolated by the exponential curve.  $\mu_0 H_c(T)$  was obtained by the relationship<sup>18</sup>

$$G_n(T) - G_s(T) = \int_T^{T_c} \frac{\Delta S(T')}{T'} dT' = \frac{\mu_0 V_m H_c(T)^2}{2}, \quad (9)$$

where  $V_m$  is the molar volume. The calculated value of  $\mu_0 H_c(0)$  is 5.72 mT for Bi<sub>2</sub>Pd<sub>3</sub>Se<sub>2</sub>. On the other hand, the BCS theory predicts the magnitude of  $\mu_0 H_c(0)$  by the relation

$$\mu_0 H_c(T) = \left[ \frac{0.47 \mu_0 \gamma T_c^2}{V_m} \right]^{1/2}. \quad (10)$$

From the obtained  $\gamma$ ,  $V_m$ , and  $T_c$  for Bi<sub>2</sub>Ni<sub>3</sub>Se<sub>2</sub>,  $\mu_0 H_c(0)$  is calculated to be 5.96 mT, and this value is close to the values from Eq. (9). Moreover, the penetration depth  $\lambda(0)$ , GL parameter  $\kappa(0)$ , and lower critical field at 0 K  $\mu_0 H_{c1}(0)$  are estimated from the relations<sup>15</sup>

$$\mu_0 H_c(0) = \frac{\Phi_0}{2\sqrt{2}\pi\lambda(0)\xi_{\text{GL}}(0)}, \quad (11)$$

$$\kappa(0) = \frac{\lambda(0)}{\xi_{\text{GL}}(0)}, \quad (12)$$

TABLE II. Superconducting and normal-state properties for Bi<sub>2</sub>Pd<sub>3</sub>X<sub>2</sub> (X=S,Se).

	Bi <sub>2</sub> Pd <sub>3</sub> S <sub>2</sub>	Bi <sub>2</sub> Pd <sub>3</sub> Se <sub>2</sub>
$V_m$ (m <sup>3</sup> /mol)	$8.62 \times 10^{-5}$	$9.09 \times 10^{-5}$
$\gamma$ (mJ/mol K <sup>2</sup> )	5.9(1)	8.3(1)
$\Theta_D$ (K)	170(1)	150(1)
$T_c^{\text{mid},R}$ (K)		0.96
$T_c^{\text{mid},C}$ (K)		0.81
$\Delta C/\gamma T_c^{\text{mid},C}$		1.15
$\mu_0 H_{c2}(0)$ (mT)		315
$\mu_0 H_c(0)$ (mT)		5.72
$\mu_0 H_{c1}(0)$ (mT)		0.38
$\xi_{\text{GL}}(0)$ (Å)		323
$\lambda(0)$ (Å)		12590
$\kappa(0)$		38.9

$$\mu_0 H_{c1} = \frac{\mu_0 H_c}{\sqrt{2}\kappa} \ln \kappa. \quad (13)$$

By using the value of  $\mu_0 H_c(0)$  obtained from Eq. (9),  $\lambda(0)$ ,  $\kappa(0)$ , and  $\mu_0 H_{c1}(0)$  are estimated to be 12 590 Å, 38.9, and 0.38 mT, respectively. These superconducting parameters are summarized in Table II. The value of  $\kappa(0)$  strongly suggest that Bi<sub>2</sub>Pd<sub>3</sub>Se<sub>2</sub> is a typical type-II superconductor.

#### IV. SUMMARY

We have investigated the transport properties of two ternary-metal-rich chalcogenides Bi<sub>2</sub>Pd<sub>3</sub>X<sub>2</sub> (X=S,Se). It is found that Bi<sub>2</sub>Pd<sub>3</sub>Se<sub>2</sub> is a superconductor with a critical temperature  $T_c$  of about 0.9 K, while Bi<sub>2</sub>Pd<sub>3</sub>S<sub>2</sub> is a normal metal down to 0.35 K. The  $\mu_0 H_{c2}(0)$  values is estimated to be about 315 mT from the midpoint temperatures of electrical resistivity under the magnetic fields. From specific heat measurements,  $\gamma$ ,  $\Theta_D$ , and  $\Delta C/\gamma T_c$  for Bi<sub>2</sub>Pd<sub>3</sub>Se<sub>2</sub> are 8.3 mJ/mol K<sup>2</sup>, 150 K, and 5.9 mJ/mol K<sup>2</sup>, respectively, and  $\gamma$  and  $\Theta_D$  for Bi<sub>2</sub>Pd<sub>3</sub>S<sub>2</sub> are 5.9 mJ/mol K<sup>2</sup> and 170 K, respectively. Study of the specific heat in the superconducting state of Bi<sub>2</sub>Pd<sub>3</sub>Se<sub>2</sub> suggests that Bi<sub>2</sub>Pd<sub>3</sub>Se<sub>2</sub> is categorized as a weak-coupling BCS, *s*-wave superconductor. The small specific heat jump is suggestive of anisotropic superconductivity.

\*wake@sci.hokudai.ac.jp

<sup>1</sup>L. Chen and J. D. Corbett, J. Am. Chem. Soc. **125**, 1170 (2003).

<sup>2</sup>A. I. Baranov, A. A. Isaeva, L. Kloo, and B. A. Popovkin, Inorg. Chem. **42**, 6667 (2003).

<sup>3</sup>B. Harbrecht and H. F. Franzen, J. Less Common Met. **113**, 349 (1985).

<sup>4</sup>M. A. Peacock and J. McAndrew, Am. Mineral. **35**, 425 (1950).

<sup>5</sup>M. Zabel, S. Wandering, and K.-J. Range, Z. Naturforsch. B **34**, 238 (1979).

<sup>6</sup>S. Natarajan and G. V. S. Rao, J. Less Common Met. **138**, 215 (1988).

<sup>7</sup>A. I. Baranov, A. V. Olenov, and B. A. Popovkin, Russ. Chem. Bull. **50**, 353 (2001).

<sup>8</sup>T. Sakamoto, M. Wakeshima, and Y. Hinatsu, J. Phys.: Condens. Matter **18**, 4417 (2006).

<sup>9</sup>T. Sakamoto, M. Wakeshima, Y. Hinatsu, and K. Matsuhira, Phys. Rev. B **75**, 060503(R) (2007).

<sup>10</sup>F. Izumi and T. Ikeda, Mater. Sci. Forum **321–324**, 198 (2000).



- <sup>11</sup>A. Clauss, *Naturwissenschaften* **64**, 145 (1977).
- <sup>12</sup>R. P. Huebener, *Phys. Rev.* **146**, 490 (1966).
- <sup>13</sup>N. R. Werthamer, E. Helfand, and P. C. Hohenberg, *Phys. Rev.* **147**, 295 (1966).
- <sup>14</sup>P. H. Pan, D. K. Finnemore, A. J. Bevolo, H. R. Shanks, B. J. Beaudry, F. A. Schmidt, and G. C. Danielson, *Phys. Rev. B* **21**, 2809 (1980).
- <sup>15</sup>M. Tinkham, *Introduction to Superconductivity*, 2nd ed. (McGraw-Hill, Singapore, 1996).
- <sup>16</sup>H. Okamoto and Y. Ishihara, *Phys. Rev. B* **48**, 3927 (1993).
- <sup>17</sup>H. Okamoto, H. Taniguti, and Y. Ishihara, *Phys. Rev. B* **53**, 384 (1996).
- <sup>18</sup>W. L. McMillan, *Phys. Rev.* **167**, 331 (1968).